

Assessment of Cell Cycle and Induction of Apoptosis by Shiga-like Toxin Produced by *Escherichia coli* O157:H7 in T47D Breast Cancer Cells Using Flow Cytometry

I Wayan Suardana^{1*}, Ida Bagus Ngurah Swacita¹, Komang Januartha Putra Pinatih², Hamong Suharsono³, Dyah Ayu Widiasih⁴

Abstract

Background: The low general toxicity against tumors expressing globotriaosylceramide (Gb3) and Shiga-like toxins produced by *E. coli* have been proposed as an anti-cancer therapy because of their specific target. This study aimed to determine the potency of the local strains of *E. coli* O157:H7 isolated from humans and cattle as a new breast cancer therapy by analyzing the cell cycle's inhibition and apoptosis induction. **Material and Methods:** Approximately 10 cultured T47D cells were subjected to Shiga-like toxin produced by four local isolates of *E. coli* O157:H7, including KL-48 (2) from humans, and SM-25 (1), SM-7 (1), DS-21 (4) from cattle. Using ATCC 43894 as a control, the treatment was observed for 24 h by two replications. In addition, a FITC-Annexin V and PI assay were used to observe apoptosis and necrosis effect, as well as to analyze the cell cycle using propidium iodide (PI) staining. **Results:** The results showed the toxicity effect of Shiga in the human T47 D cells line. The viability of the cells is subjected to Shiga-like toxins produced by KL-48 (2), SM7 (1), ATCC 43894, SM-25 (1), and DS-21 (4) isolates decreased with 15.20, 16.36, 22.17, 22.64, and 33.86%, in contrary to control of 94.36%. These were supported by the cells entering the late apoptosis of the cell cycle through each isolate with 67.66, 62.60, 63.68, 63.90, and 54.74%, and a control of 0.01%. Also, the necrosis cell for each treatment of 12.73, 19.3, 10.84, 10.53, and 4.86% was higher than the control of 5.51%. These were confirmed by the higher percentage of the cells treated with toxins of KL-48 (2), SM7(1), ATCC 43894, SM-25 (1), and DS-21 (4), which entered G0-G1 of the cell cycle phase with 66.41, 63.37, 61.52, 55.36, and 47.28%, respectively, than control of 40.69%. Additionally, the toxicity effect was supported by an increase in the cells entering the S and the G2-M phase of the cycle for each treatment. **Conclusion:** It is concluded that the Shiga-like toxin produced by *E. coli* O157:H7 local isolates can be developed as a drug against breast cancer based on its effect to arrest induction of the cell cycle and inducing apoptosis.

Keywords: Apoptosis- breast cancer- *E. coli* O157:H7- necrosis- Shiga-like toxin

Asian Pac J Cancer Prev, 23 (10), 3247-3252

Introduction

Shiga toxin *Escherichia coli* (STEC) is a significant public health problem in developed and developing countries due to the severity of the diseases they cause (Karmali et al., 2010). On the other hand, it can be used for medical purposes such as cancer therapy (Bergan et al., 2012). This phenomenon results from its capability to inactivate multiple cell stress signaling pathways, which may result in apoptosis, autophagy, or activation of the innate immune response (Lee et al., 2016).

Scientific studies showed that the Shiga-like toxin

produced by *E. coli* O157:H7 induces apoptosis in specific cells and is infected by this bacterium (Fujii et al., 2003). Apoptosis is an essential multi-step process in eliminating damaged or abnormal cells (Choi and Kim, 2009). Therefore, the essential targets in cancer therapy strategy are apoptosis and cell cycle arrest inductions (Doucas et al., 2006).

The low general toxicity against tumors expressing globotriaosylceramide (Gb3) and Shiga-like toxins produced by *E. coli* has been proposed as an anti-cancer therapy because of their specific target (Frankel et al., 2000). On the other hand, the Gb3 receptor is highly

¹Department of Preventive Veterinary Medicine, Faculty of Veterinary Medicine, Udayana University. Jl. P.B. Sudirman, Denpasar-Bali. 80234. Indonesia. ²Department of Clinical Microbiology, Faculty of Medicine, Udayana University. Jl. P.B. Sudirman, Denpasar-Bali. 80234. Indonesia. ³Department of Basic Veterinary Medicine, Faculty of Veterinary Medicine, Udayana University. Jl. P.B. Sudirman, Denpasar-Bali. 80234. Indonesia. ⁴Department of Veterinary Public Health, Faculty of Veterinary Medicine, Gadjah Mada University. Jl. Fauna No. 2 Karangmalang, Yogyakarta 55281 Indonesia. *For Correspondence: wayan_suardana@unud.ac.id

expressed on the surface of several tumor cells lines, such as breast cancer (Garipey, 2001). Remarkably, many cancer cells overexpress Gb3 on their surface, thereby enabling the binding of toxins or the non-toxic pentameric Stx B-subunits related to anti-cancer agents (Maak et al., 2011). The previous study by Suardana et al. (Suardana et al., 2018) stated that the local isolates from humans and cattle have similar sequences of *stx2* gene with ATCC 43894 as control but produced lower toxicity. It evaluated the potency of Shiga-like toxin produced by the local isolates of *E. coli* O157:H7 as a novel agent to enhance apoptosis and necrosis in the human T47D cells line.

Materials and Methods

Ethical approval

The Institutional Animal Ethics Committee approval was not required to conduct this study since no live animals were used.

Cultivation of Escherichia coli O157:H7 isolates

The five local isolates of *E. coli* O157:H7, KL-48 (2) from humans and cattle, such as SM-25 (1), SM-7 (1), DS-21 (4), and ATCC 43894 control, respectively, were cultivated by aerobically culturing lactose broth medium (LB) at 37°C overnight. According to the previous method, the presumptive isolates were re-confirmed using the *E. coli* O157 latex agglutination test (Oxoid, DR120M) (Suardana, 2014; Suardana et al., 2015).

Isolation of Shiga-like toxin

The Shiga-like toxin of five isolates was cultured on *Luria Bertani*/LB broth (Sigma, L3022). There were then incubated at 37°C for 24 h before being centrifugated at 2000 rpm for 40 min at 4°C. Subsequently, approximately 5.97g of ammonium sulfate (Sigma, A4418) was gradually added to 15 ml of the supernatant to obtain 65% saturation. The solutions were re-centrifugated at 2000 rpm for 40 min, and each precipitate was diluted with 3 ml of sterile physiological saline before it was dialyzed at 4°C overnight. Each toxin was sterilized using 0.22 µm filters (Corning, 431 219). Finally, the concentration was measured (Suardana et al., 2010; Suardana et al., 2016).

Preparation of human T47D cancer cell

The monolayer culture of human T47D was performed by culturing one ml of the cell maintained under standard conditions at the LPPT laboratory, Gadjah Mada University, in complete Dulbecco's Modified Eagle Medium (DMEM) (Sigma, D6046). In addition, these media were supplemented with 100 IU penicillin/ml, 100 mg/ml Streptomycin, 50 µg fungizon (Fisher Scientific, BW17-745H), and 10% Newborn Calf Serum (Sigma N4887). The cell was then incubated in a humidified atmosphere containing 5% CO₂ at 37°C.

Toxicity assay

Up to 50 µL of T47D cells were implanted into each well of 96 microplates (Merck) and then incubated in 5% CO₂ for 24 h to obtain confluent growth at

a density of 5 x 10⁴ cells/well. The media were replaced, after which 50 µL of the serially diluted crude toxin was added. Subsequently, the crude toxin was removed, and monolayer cells were washed two times after being incubated for 15 min at room temperature. A complete growth medium of 100 µL was added to the cells before incubating for 24 h at 37°C, with 5% CO₂. The cells were then washed with phosphate buffer saline (PBS) solution. Furthermore, 10 and 100 µL of MTT reagent (3-(4, 5 dimethyliazol-2-yl) -2.5-diphenyl tetrazolium bromide) 0.5% and culture media were added to each well, respectively. Incubation was performed overnight at 37°C for 4-6 h in 5% CO₂ to form formazan, and the reaction was stopped by adding 100 µL of MTT reagent stopper. An ELISA reader analyzed this at λ 550 nm (Suardana et al., 2010; Suardana et al., 2018).

Cell apoptosis and necrosis assay

Apoptosis of T47D cells was determined according to the previous method with slight modification (Vermes et al., 1995; Liu et al., 2018). It was assessed using FITC-Annexin V and PI method (Invitrogen; Thermo Fisher Scientific, Inc.). Briefly, 1×10⁶ human T47D cells were harvested, washed twice with cold PBS by centrifugation at 2000 rpm for 5 min, and resuspended in 100 µL binding buffer (Thermo Fisher Scientific, Inc.). A total of 100 µL Annexin V-fluorescein isothiocyanate and 2 µL PI were added to the solution, following 10 min incubation in the dark at room temperature. The binding buffer of 400 µL was added to the solution, and cells were analyzed using the Accuri™ C6 Flow Cytometer. The results were processed using CellQuest™ software 1.0 (BD Biosciences).

Cell cycle analysis with propidium iodide staining

The cell cycle analysis was performed according to the previous method with slight modification (Johansson et al., 2009). The human T47D cells with a density of 7 x 10⁵ were isolated locally upon completion of 24 h incubation with/without IC₅₀ of each Shiga-like toxin local isolate and control ATCC 43894. The cell cultures were washed with PBS before being treated with 0.1% trypsin at 37°C. Its suspension was collected and washed with PBS (2000 rpm, 5 min). The cell was resuspended for 30 min at 4°C in cold PBS containing 70% absolute ethanol for fixation and permeabilization of the membrane. Subsequently, the cells were washed twice and treated with 40 µg/mL. They were rinsed in PBS for 15 min at 37°C (final volume 100 ml). Finally, 2 µl of PI staining solution was added, followed by incubation in the dark at room temperature for 10 min. PI fluorescence was measured at 488 nm, and a Fluorescence Activated Cell Sorter analyzed the cell cycle. Approximately ten thousand cells were observed in each experiment, and the percentage of cell cycle arrest in the G0/G1, S, and G2/M phases was measured.

Results

Toxicity assay

Results of the toxicity assay showed that the viable or deleterious T47D cells were different from each treatment

and control (Figure 1).

The IC₅₀ value of Shiga-like toxin produced by *E. coli* O157:H7 human strain KL-48 (2) was almost equal to control ATCC 43894. The toxin concentration required for 50% in vitro inhibition of ATCC 43894 and KL-48 (2) is almost similar at 0.92 and 0.94 ug/mL, respectively. Furthermore, other isolates from cattle, such as SM-25 (1), SM-7 (1), and DS 21 (4), required higher concentrations at 1.08, 1.03, and 1.03 ug/mL, respectively.

Cell apoptosis assay

Apoptosis and necrosis as toxic effects of Shiga were analyzed using FITC-Annexin V and PI methods. Figure 2 shows the test description of intact (FITC-/PI-), apoptotic ((FITC+/PI-), and necrotic cells (FITC+/PI+) (Vermees et al., 1995).

Figure 2 shows viable apoptosis, late apoptosis, and necrosis of the human T47D cells cycle after 24 h of incubation. The lowest percentage of viable cells was shown in those treated with KL-48 (2), SM 7 (1), ATCC 43894, SM-25 (1), DS-21 (4) toxins, and control of 15.20, 16.36, 22.17, 22.64, 33.86, and 94.36%, respectively. On the other hand, cells at 67.66, 62.60, 63.68, 63.90, and 54.74% entered late apoptosis higher than the control 0.01%. Also, the cells expected to be necrosis for each treatment were higher at 12.73, 19.3, 10.84,

10.53, and 4.86% than control at 5.51%. These results show the tendency towards deleterious effects of Shiga-like toxin. Previous studies reported an equal effect of Shiga-like toxin on breast cancer tissue (Cherla et al., 2003; Johansson et al., 2009).

Cell cycle analysis

Figure 3 shows the contour diagram of T47D cells' cycle with and without being treated with Shiga-like toxin. Table 1 represents the summary of each cycle entering the G0-G1, S, and G2-M phases.

Table 1 shows various effects of the toxin on the cell cycle arrest. The highest effect on the cell cycle arrest in the G0-G1 phase was shown by the cell treated with KL-48 (2) toxin. Furthermore, the overall percentages of cells in the G0-G1 phase were 66.41, 63.37, 61.52, 55.36, and 47.28% for T47D cells treated with toxins of KL-48 (2), ATCC 43894, SM 25 (1), SM 7 (1), and DS 21 (4), respectively. The results differed from T47D cell control without toxin treatment, which showed the highest percentage of the G2-M as the active phase preparing cells for division (mitosis).

Discussion

This study showed that the T47D cells that enter

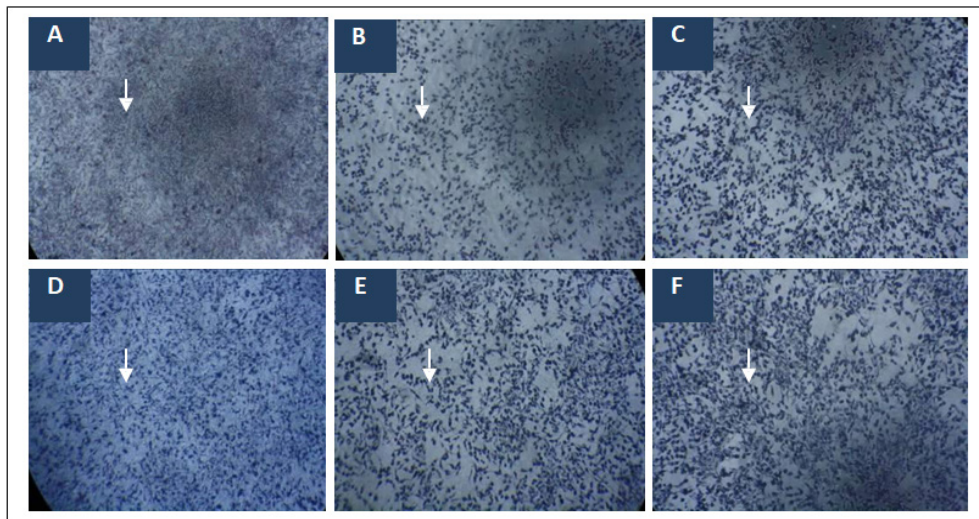


Figure 1. Staining of T47D Cells with MTT 24 Hours Post-treatment. The arrow (→) indicates live cells stained. A, control cells without treatment; B, cells treated by the toxin *E. coli* ATCC 43894 as a positive control; C, Cells treated by KL-48 toxin (2); D, Cells treated by SM-25 toxin (1); E, Cells treated by SM7 toxin (1) and F, Cells treated by DS-21 toxin (4) as a negative control.

Table 1. Percentage of T47D Cells with each Cell Cycle Arrest after 24 h Treated /without Shiga-like Toxin with Inhibitory Concentration 50 (IC₅₀)

Treatments	Percentage of T47D cell cycle after treatments		
	GO-G1	S-phase	G2-M
T47D control cell (without toxin)	40.69	22.56	42.3
T47D cell + ATCC 4389 toxin	63.37	17.58	19.06
T47D cell + KL-48 (2) toxin	66.41	17.1	16.61
T47D cell + SM 25 (1) toxin	61.52	20.14	18.35
T47D cell + SM 7 (1) toxin	55.36	25.33	19.25
T47D cell + DS 21 (4) toxin	47.28	22.95	29.71

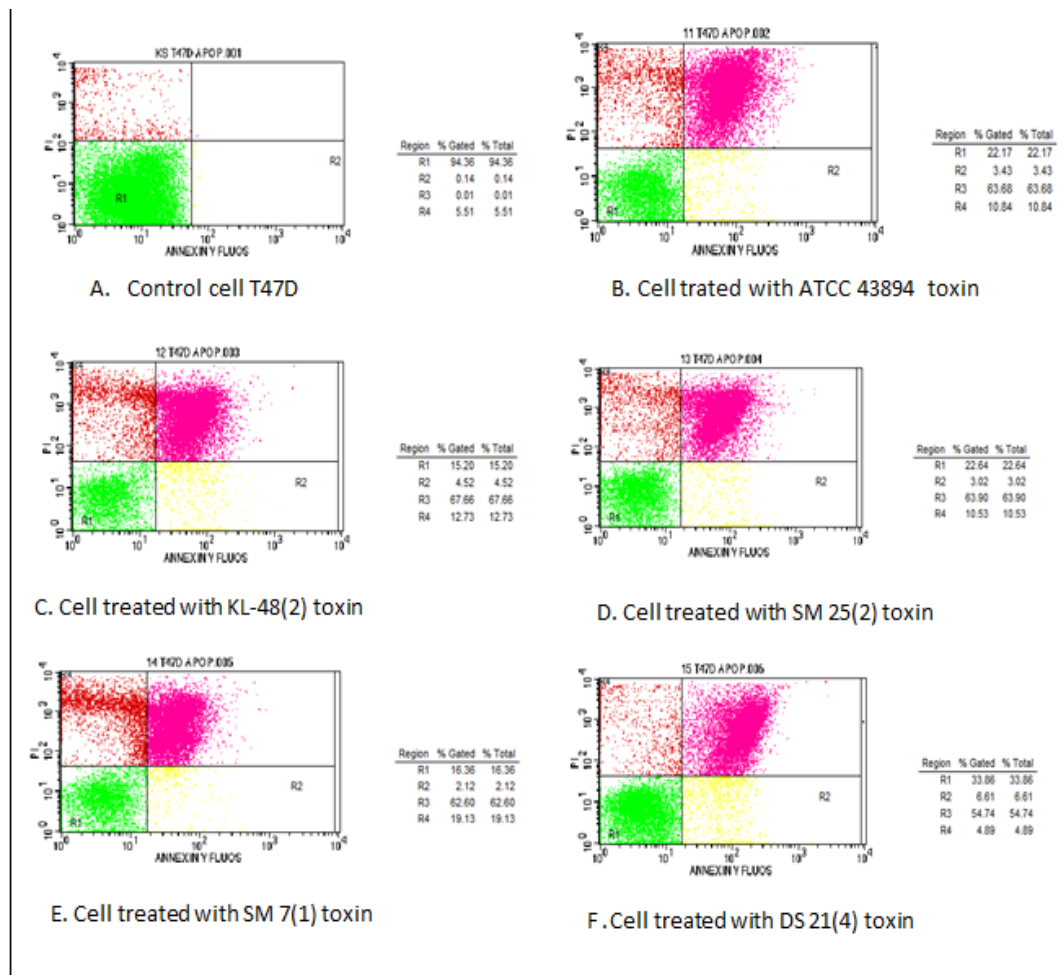


Figure 2. Contour Diagram of FITC-Annexin V/PI Flow Cytometry of T47D Cell Line with and without Treated by Shiga-like Toxin. The lower left quadrants of each panel show the viable cells, which exclude PI and are negative for FITC-Annexin V binding. The upper right quadrants (R1) contain the non-viable, necrotic cells, positive for FITC-Annexin V binding and PI uptake. The lower right quadrants (R2) represent the apoptotic cells, FITC-Annexin V positive and PI negative, demonstrating cytoplasmic membrane integrity.

the stages of apoptosis, late apoptosis, and necrosis were activated by applying the Shiga-like toxin. T-test analysis of a sample showed that the mean of toxin-treated cells experienced a significant decrease ($P < 0.05$) in the number of viable cells with an average of 22.045 (+ 7.4), 95% CI, 12.86 - 31.23 compared with those without treatment of 94.36 %. This result was confirmed by a significant increase ($P < 0.05$) of the cells entering the early apoptotic stage with a mean of 3.94 (+1.72), 95% CI, 1.80-6.08) compared with a control of 0.14%. The number of cells entering the final stage of apoptosis was also significantly higher ($P < 0.05$) in the toxin treatment with an average of 62.52 (+4.75), 95% CI 56.62-68.41 compared to control of 0.01%. Similarly, cells with necrosis experienced an increase from 5.51% in control to 11.62 (+ 5.12), 95% CI, 5.27 - 17.98, which was not statistically significant ($P > 0.05$). This study reinforces the previous result, which discovered the apoptosis effect of Shiga-like toxin produced by KL-48 (2) human and SM-25 (1) cattle in T47D cell line at 80.3, and 50.3% and their necrosis effect of 8.0, and 13.0%, respectively. Furthermore, these were tested by acridine orange/ethidium bromide double staining (Putra Pinatih et al., 2021). Previous studies showed that apoptosis was

induced rapidly (60%) in HeLa cells after exposure to Shiga toxin within 4 hours (Fujii et al., 2003). These studies supported previous claims mentioning Shiga-like toxins as cancer therapy (Endo et al., 1988).

These results align with the study conducted by Johansson et al. (Johansson et al. 2009), which stated the therapeutic agent against malignant tumors, including breast cancer cells of bacterial toxins such as verotoxin. It is known that all members of the Stx family are composed of 1A and 5B subunit proteins. The A subunit is an N-glycosidase that removes adenine 4342 of 28S RNA of the 60S ribosomal subunit (Endo et al., 1988), rendering ribosomes inactive for protein synthesis (Obrig et al., 1987). Furthermore, Stx1B induces apoptosis with accompanying DNA fragmentation, whereas the Stx1A is discovered to be necrotic with no DNA fragmentation (Nakagawa et al., 1999; Kojio et al., 2000).

Generally, Stx activates caspases 3, 6, 8, and 9 as essential proteins for the apoptosis of cancer cells (Ashkenazi and Dixit, 1998). The caspase 8 is known as Bid activation, an endogenous protein known to permeabilize mitochondrial membranes. The cleavage of Bid will convert its form from inactive 26 kDa to an active 15 kDa, capable of disrupting the mitochondrial

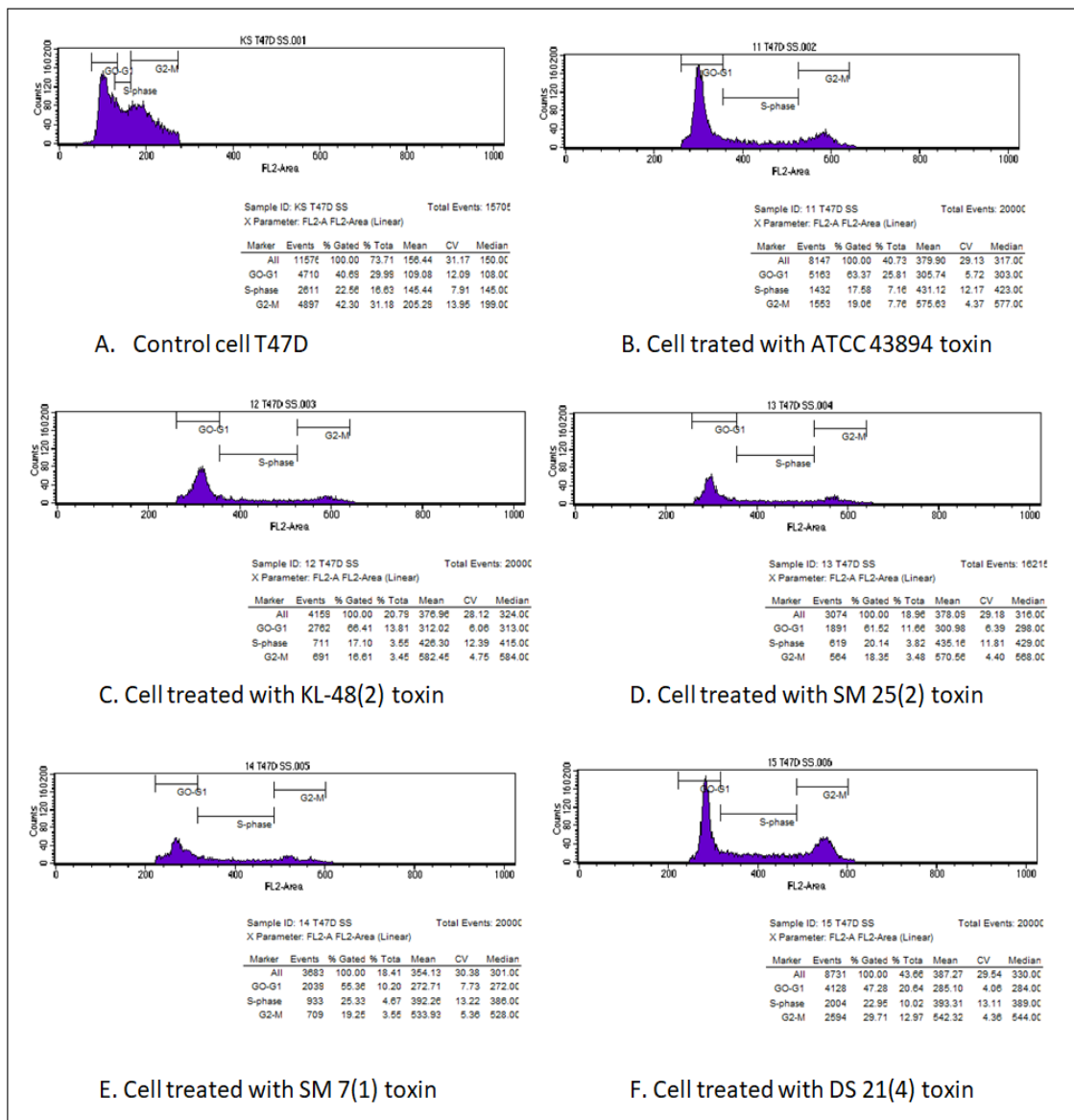


Figure 3. Contour Diagram of T47D Cell Cycle after 24 h Treated by and without Shiga-like Toxin

outer membrane. This activity induces the release of C cytochrome from the mitochondria. In addition, it triggers the activation of caspase-9, which then accelerates apoptosis by activating 3 (Green and Reed, 1998).

Table 1 shows the cell cycle arrest of the T47D cell line in the G0-G1 phase, except for DS-21 (4). The lowest effect was observed after being treated with Shiga-like toxin of ATCC 43894, KL-48 (2), SM-25 (1), and SM-7 (1). Cell cycle analysis presented in Table 1 shows a simultaneous effect on the cytotoxic assay. The analysis of the one-sample T-test showed that the cell cycle among treatments was significantly increased ($P < 0.05$) in the mean of cells entering the G0-G1 phase, which was 58.79 (+ 7.60), 95% CI 49.36-68.22 compared to those that receive no toxin treatment 40.69%. The increase in the number of cells retained in the G0-G1 phase was confirmed by a decrease of those entering the S phase by 20.62 (+ 3.52) 95% CI, 16.25-24.99. A significant decrease ($P < 0.05$) was observed in the number of cells entering the G2-M phase. The cells treated with Shiga-like toxin showed a mean of 20.60 (+ 5.20), 95% CI, 14.14-27.05,

which was much lower than the control at 42.30%. The result is supported by several articles which have presented correlations between DNA ploidy classification, cell cycle variables, and clinical pathologic variables (Bergers et al., 1996). The reliability of the flow cytometry method to detect cell cycle phases and similar phenomena was discovered. A decrease in leukemic cells in the S, G2, and M phases was accompanied by an increase in G1 (Vignon et al., 2013). Furthermore, an accumulation of the cell in the G2+M phase was accompanied by a decrease in the G0 + G1 population (Morris et al., 1993). This result is in line with the potency of verotoxin for the treatment of breast cancer. It was showed that verotoxin-1 is sensitive to cytotoxicity, caspase activation, and DNA activation of human T47D cells, which are highly expressive Gb3 (Johansson et al., 2009). The results show the deleterious effect of Shiga-like toxin produced by local isolates of *E. coli* O157:H7, specifically KL48 (2) human T47D cells. These represent the potency of this toxin as a promising drug against breast cancer.

Author Contribution Statement

IWS: conceived, designed, and supervised the study, DAW and KJPP: performed laboratory analysis, IBNS and HS: Analyzed the data and wrote and edited the final manuscript. All authors read and approved the final manuscript.

Acknowledgments

The authors are grateful to Prof. Dr. Supar, MS., for his provision of *E. coli* ATCC43894 controls isolate.

Funding

This study was supported by a research grant from the Ministry of Research, Technology and Higher Education of Indonesia in “the Competitions Grant,” providing financial support with contract no. No. 415.75/UN.14.4.A/PL/2017. Mart, 30th 2017.

Conflict of Interests

The authors declare that they have no conflict of interest.

References

Ashkenazi A, Dixit VM (1998). Death receptors: signaling and modulation. *Science*, **281**, 1305-8.

Bergan J, Dyve Lingelem AB, Simm R, et al (2012). Shiga toxins. *Toxicon*, **60**, 1085-107.

Bergers E, van Diest PJ, Baak JP (1996). Cell cycle analysis of 932 flow cytometric DNA histograms of fresh frozen breast carcinoma material. Correlations between flow cytometric, clinical, and pathologic variables. MMMCP Collaborative Group. Multicenter Morphometric Mammary Carcinoma Project Collaborative Group. *Cancer*, **77**, 2258-66.

Cherla RP, Lee SY, Tesh VL (2003). Shiga toxins and apoptosis. *FEMS Microbiol Lett*, **228**, 159-66.

Choi EJ, Kim GH (2009). Apigenin Induces Apoptosis through a Mitochondria/Caspase-Pathway in Human Breast Cancer MDA-MB-453 Cells. *J Clin Biochem Nutr*, **44**, 260-5.

Doucas H, Garcea G, Neal CP, et al (2006). Chemoprevention of pancreatic cancer: a review of the molecular pathways involved, and evidence for the potential for chemoprevention. *Pancreatology*, **6**, 429-39.

Endo Y, Tsurugi K, Yutsudo T, et al (1988). Site of action of a Verotoxin (VT2) from *Escherichia coli* O157:H7 and of Shiga toxin on eukaryotic ribosomes. RNA N-glycosidase activity of the toxins. *Eur J Biochem*, **171**, 45-50.

Frankel AE, Kreitman RJ, Sausville EA (2000). Targeted toxins. *Clin Cancer Res*, **6**, 326-34.

Fujii J, Matsui T, Heatherly DP, et al (2003). Rapid apoptosis induced by Shiga toxin in HeLa cells. *Infect Immun*, **71**, 2724-35.

Garipey J (2001). The use of Shiga-like toxin I in cancer therapy. *Crit Rev Oncol Hematol*, **39**, 99-106.

Green DR, Reed JC (1998). Mitochondria and apoptosis. *Science*, **281**, 1309-12.

Johansson D, Kosovac E, Moharer J, et al (2009). Expression of verotoxin-1 receptor Gb3 in breast cancer tissue and verotoxin-1 signal transduction to apoptosis. *BMC Cancer*, **9**, 67.

Karmali MA, Gannon V, Sargeant JM (2010). Verocytotoxin-producing *Escherichia coli* (VTEC). *Vet Microbiol*, **140**, 360-70.

Kojio S, Zhang H, Ohmura M, et al (2000). Caspase-3 activation and apoptosis induction coupled with the retrograde transport of Shiga toxin: inhibition by brefeldin A. *FEMS Immunol Med Microbiol*, **29**, 275-81.

Lee MS, Koo S, Jeong DG, et al. (2016). Shiga Toxins as Multi-Functional Proteins: Induction of Host Cellular Stress Responses, Role in Pathogenesis and Therapeutic Applications. *Toxins (Basel)*, **8**.

Liu L, Liu Z, Wang H, et al (2018). 14-3-3beta exerts glioma-promoting effects and is associated with malignant progression and poor prognosis in patients with glioma. *Exp Ther Med*, **15**, 2381-7.

Maak M, Nitsche U, Keller L, et al (2011). Tumor-specific targeting of pancreatic cancer with Shiga toxin B-subunit. *Mol Cancer Ther*, **10**, 1918-28.

Morris SM, Domon OE, McGarrity LJ, et al (1993). Flow cytometric analysis of the cell-cycle distribution of spleen lymphocytes isolated from Fischer 344 rats exposed to ethyl nitrosourea. *Cell Biol Toxicol*, **9**, 77-83.

Nakagawa I, Nakata M, Kawabata S, et al (1999). Regulated Shiga toxin B gene expression induces apoptosis in mammalian fibroblastic cells. *Mol Microbiol*, **33**, 1190-9.

Obrig TG, Moran TP, Brown JE (1987). The mode of action of Shiga toxin on peptide elongation of eukaryotic protein synthesis. *Biochem J*, **244**, 287-94.

Putra Pinatih KJ, Suardana IW, Widiasih DA, et al (2021). Shiga-Like Toxin Produced by Local Isolates of *Escherichia coli* O157:H7 Induces Apoptosis of the T47D Breast Cancer Cell Line. *Breast Cancer Basic Clin Res*, **15**, 1-7.

Suardana IW (2014). Analysis of Nucleotide Sequences of the 16S rRNA Gene of Novel *Escherichia coli* Strains Isolated from Feces of Human and Bali Cattle. *J Nucleic Acids*, **2014**, 475754.

Suardana IW, Artama WT, Asmara W, et al (2010). Adherence pheno-genotypic of *Escherichia coli* O157:H7 isolated from beef, feces of cattle, chicken, and humans. *Ind J Biotech*, **16**, 46-52.

Suardana IW, Pinatih KJ, Widiasih DA, et al (2016). Regulatory elements of *stx2* gene and the expression level of Shiga-like toxin 2 in *Escherichia coli* O157:H7. *J Microbiol Immunol Infect*, **2016**.

Suardana IW, Pinatih KJP, Widiasih DA, et al (2018). Regulatory elements of *stx2* gene and the expression level of Shiga-like toxin 2 in *Escherichia coli* O157:H7. *J Microbiol Immunol Infect*, **51**, 132-40.

Suardana IW, Widiasih DA, Mahardika IGNK, et al (2015). Evaluation of zoonotic potency of *Escherichia coli* O157:H7 through arbitrarily primed PCR methods. *Asian Pac J Trop Biomed*, **5**, 915-20.

Vermes I, Haanen C, Steffens-Nakken H, et al (1995). A novel assay for apoptosis. Flow cytometric detection of phosphatidylserine expression on early apoptotic cells using fluorescein-labeled Annexin V. *J Immunol Methods*, **184**, 39-51.

Vignon C, Debeissat C, Georget MT, et al (2013). Flow cytometric quantification of all cell cycle phases and apoptosis in a two-color fluorescence plot. *PLoS One*, **8**, e68425.



This work is licensed under a Creative Commons Attribution-Non Commercial 4.0 International License.